J|A|C|S COMMUNICATIONS

Published on Web 01/26/2006

Cytochrome Display on Amyloid Fibrils

Andrew J. Baldwin,[†] Reto Bader,[†] John Christodoulou,[†] Cait E. MacPhee,[§] Christopher M. Dobson,*[,†,§] and Paul D. Barker*[,†]

Department of Chemistry, University of Cambridge, Lensfield Road, Cambridge, CB2 1EW, U.K., and Department of Physics, University of Cambridge, Cavendish Laboratory, Madingley Road, Cambridge, CB3 0HE, U.K.

Received September 24, 2005; E-mail: pdb30@cam.ac.uk; cmd44@cam.ac.uk

Protein amyloid fibrils have many features that are potentially of great value for the construction of functional materials.[1−4] For example, they self-assemble from soluble precursors and once formed are chemically and physically stable, with a uniform architecture. These properties have recently been used to template the formation of metal nanowires,[2,3] and enzymes and GFP have been successfully attached in their active forms to amyloid fibrils.[5,6] Many of nature's molecular wires consist of chains of heme molecules organized optimally for electron transfer over long (∼10 nm) distances.[7] The display of redox proteins on fibrils would mimic such multiheme cytochromes and hence could provide materials for self-assembling molecular wires and circuits. Toward this end, we show here that we can successfully display a porphyrin binding protein on an amyloid fibril scaffold and incorporate heme to form a functional *b*-type cytochrome.

Amyloid fibrils can be formed from a large variety of polypeptide sequences.[8] They have diameters typically around 10 nm and lengths often exceeding several micrometers. They share a common X-ray fiber diffraction pattern indicative of β-strands perpendicular to the fibril axis. Our design of a fibrillar cytochrome sequence consists of two covalently fused sections. The first is a tandem repeat of an 86 residue SH3 domain, $(SH3)_2$, which forms well-defined fibrils at concentrations as low as 30 μM in 6 h under appropriate conditions.[9] The second is a functional metalloporphyrin binding unit, the 106 residue cytochrome b_{562} from *E. coli*, which by itself does not aggregate on the same time scale under the conditions required for fibril formation by $(SH3)_2$.

We constructed a gene for a 294 residue, 32 kDa protein, $(SH3)_2$Cyt, which fused the cytochrome (Cyt) to the C-terminus of the tandem repeat via a 6 amino acid linking sequence (GSGGGG). $(SH3)_2$Cyt was expressed in *E. coli* and holo- (heme bound) and apo-proteins were purified as described in the Supporting Information. Fibrils were formed from apo-$(SH3)_2$Cyt at pH 2 in 4 days, following an incubation for 15 min at pH 3.5 that acts to reduce the lag phase.[9] The yields of conversion of monomeric protein into aggregated material were 70−90%, as quantified by absorption at 278 nm after ultracentrifugation. The fibrils were shown to contain full length, nonhydrolyzed polypeptide by gel electrophoresis and ESI-mass spectrometry after dissociation in SDS (see Supporting Information).

The CD spectrum (Figure 1D) shows that $(SH3)_2$Cyt has an $\alpha\beta$ conformation at pH 7, initially appears unfolded at pH 2, and then tends toward a β-sheet conformation as fibrils form. The diffraction patterns (Figure 1C) of $(SH3)_2$ fibrils and apo-$(SH3)_2$Cyt fibrils both show a meridonal reflection at 4.7 Å and an equatorial reflection at 9.6 Å, characteristics of a cross-β structure. The fibrils bind thioflavin-T, give apple green birefringence on binding congo red, and show resistance to proteolysis, all indicators of an amyloid core structure.

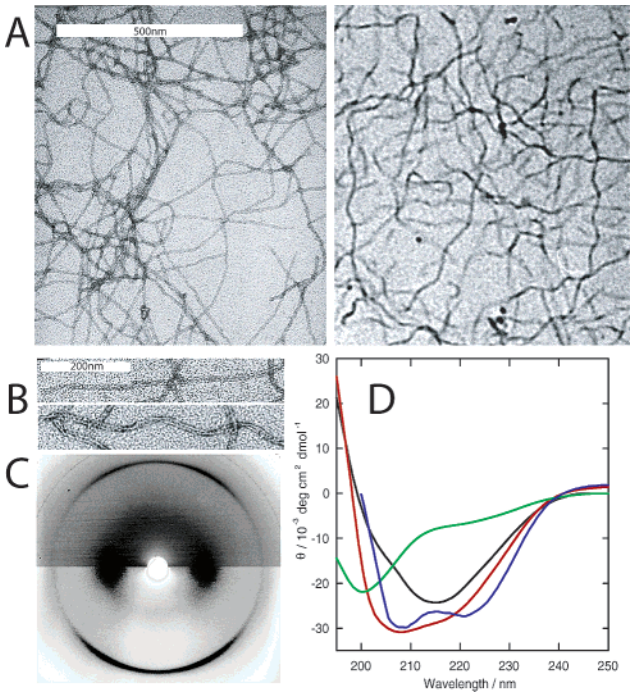

Figure 1. (A) Bright field negatively stained TEM images of $(SH3)_2$ fibrils (left) and holo-$(SH3)_2$Cyt fibrils (right). Differences in morphology are highlighted in (B), where representative $(SH3)_2$ fibrils (top) are compared to $(SH3)_2$Cyt fibrils (bottom). (C) Fiber XRD patterns taken from $(SH3)_2$ fibrils (bottom) and apo-$(SH3)_2$Cyt fibrils (top); both share meridonal and equatorial reflections and so have similar protofilament structures. (D) CD spectra. Monomeric apo-$(SH3)_2$Cyt at pH 7 has an $\alpha\beta$ structure (blue). At pH 2.3, it is unfolded (green). After $(SH3)_2$Cyt fibrils are formed, increased ellipticity at 216 nm is observed (red), consistent with the formation of β-sheets. When compared with $(SH3)_2$ fibrils (black), increased ellipticity at 222 and 208 nm is observed, suggesting additional α-helical content.

When viewed by TEM it is clear that discrete $(SH3)_2$ fibrils possess a linear, rod-like morphology (Figure 1A, left) with a 7.5 nm diameter. Discrete $(SH3)_2$Cyt fibrils have a diameter of ca. 8 nm and have a helical twist with a pitch of ca. 200 nm (Figure 1A, right). These two morphologies are compared more closely in Figure 1B. Despite sharing XRD reflections (Figure 1C) and CD spectra (Figure 1D), and hence similar core protofilaments, the higher order assembly is evidently perturbed by the addition of the cytochrome.

Cytochrome b_{562} binds metalloporphyrins noncovalently, yielding distinctive peaks in the electronic spectrum, originating from two porphyrin $\pi-\pi^*$ transitions[10] that allow a clear distinction to be made between bound and free porphyrin states. The UV-vis spectra of purified $(SH3)_2$Cyt fibrils bound to iron(II) and iron(III) protoporphyrin IX are identical to those of the wild type cytochrome within the certainty of the concentration estimate (Figure 2A,B).

[†] Department of Chemistry.
[§] Department of Physics.

10.1021/ja0565673 CCC: $33.50

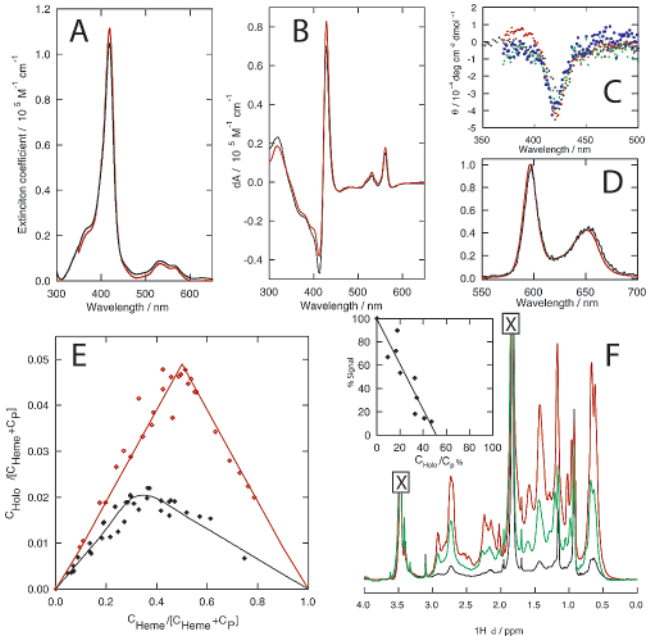

Figure 2. (A) The extinction coefficient of the wild type cytochrome (red) matches that of the fibrils (black) when bound to iron(III) porphyrin. (B) Reduced minus oxidized spectra of the heme containing cytochrome (red) and the fibrils (black). (C) CD spectra in the Soret region of reduced and oxidized cytochrome (black/red) or fibrils (green/blue). (D) The normalized emission spectra of the wild type cytochrome (red) match that of the fibrils (black) when bound to zinc(II) porphyrin and excited at either the B- or Q-bands. (E) Equilibrium heme binding data summarized as a Job plot, with monomer (10 μM) at pH 7 (red) and fibrils (10 μM) at pH 3 (black). (F) One-dimensional ^{1}H NMR spectra of apo-$(SH3)_2$Cyt fibrils (red), 25% holo (green), and 47% holo (black), showing decreasing intensity of protein signals with heme binding. Sample concentrations were 40−60 μM. Signals marked X arise from residual buffer. Inset: normalized integrated intensity (0−1.6 ppm) as a function of the percent of holo-protein to total protein.

The redox difference spectrum of heme bound to the fibrils is identical to that of the wild type cytochrome, as shown in Figure 2B. The weak Cotton effects observed in the CD spectra at the wavelengths of the Soret band (Figure 2C) are also unperturbed by fibril formation. The emission spectrum of zinc protoporphyrin IX bound to purified $(SH3)_2$Cyt fibrils, after excitation at either its B- or Q-bands (Figure 2D), is also identical to that seen for the wild type cytochrome. The rate of porphyrin binding to the $(SH3)_2$Cyt fibrils is ca. 4-fold slower than that to the wild type cytochrome. The morphology of the $(SH3)_2$Cyt fibrils observed by TEM is not detectably altered by porphyrin binding, and metalloporphyrins are not observed to bind to $(SH3)_2$ fibrils. On repurification of porphyrin bound $(SH3)_2$Cyt fibrils by ultracentrifugation, red coloration is completely localized in the pellet, showing that the cytochrome binding fraction is attached to a species of much higher molecular mass. Furthermore, NMR experiments on the fibrils (see below) show resonances arising from a species whose translational diffusion coefficient corresponds to that of a species attached to a high molecular mass particle.[11]

The extinction coefficients of the protein at 278 nm in both monomeric and fibrillar states are identical (as determined from concentrations obtained by amino acid analysis), allowing the ratio of bound heme to protein in the fibrils to be evaluated as a function of added heme (Figure 2A). The data were analyzed as described in the Supporting Information and are summarized by the Job plot in Figure 2E. The dissociation constant, K_D, of monomeric $(SH3)_2$-Cyt/heme at pH 7 is in the nanomolar range. For $(SH3)_2$Cyt fibrils at pH 3, K_D is 180 ± 30 nM. The measured ratio of heme bound per cytochrome molecule at saturation is 0.50 ± 0.04 for the fibrils. By contrast, monomeric $(SH3)_2$Cyt can be completely saturated under these conditions, showing that only half of the total heme binding sites are accessible in the fibrillar state.

Taking the fibril to be a cylinder of 8 nm diameter and of constant partial specific volume, 0.73 cm^3 g^{-1},[12] the density of metalloporphyrin molecules, and hence metal ions, can be estimated to be 2.6 per nm (see Supporting Information). This number is exceptionally high and is consistent with the observation by TEM that no individual cytochrome molecules are resolved on the surface of the fibril. The effective concentration of heme then becomes ca. 20 mM and increases the probability that the porphyrins are within the 1.4 nm limit of separation required for rapid electron transfer in biological conductors.[13]

One-dimensional ^{1}H NMR spectra (Figure 2F) of apo-$(SH3)_2$Cyt fibrils show well-resolved peaks characteristic of a mobile, unfolded protein that are not observed in spectra from the $(SH3)_2$ fibrils. The observed resonances arise from the apo-cytochrome attached to the fibril and disappear progressively upon adding heme until at 0.5 molar equiv they are no longer visible (Figure 2F, inset). These NMR data indicate that the apoprotein attached to the fibrils has extensive motional freedom but that once heme is bound, the folded cytochrome in the fibril is motionally restricted and shows resonances too broad to be detected.

In summary, we have demonstrated quantitatively that very high densities of metalloporphyrins can be displayed on the surface of an amyloid fibril formed from a rationally designed, self-assembling polypeptide fusion protein. The reproducibility and stoichiometric character of the system suggests that further investigations could provide important insights into the nature of the amyloid structure and assembly process. In addition, these fibrils provide a novel nanostructured material for the study of charge transfer in molecular systems and will facilitate initial exploration of such systems for technological applications.

Acknowledgment. We acknowledge financial support from the MRC (A.J.B.), the Wellcome Trust (C.M.D. and J.C.), the SNF (R.B.), Leverhulme Trust (C.M.D.), and the BBSRC (P.D.B.), and thank Ben Luisi, Jeremy Skepper, Mark Welland, and the IRC in Nanotechnology for support and encouragement.

Supporting Information Available: Experimental details of cloning, expression, fibril formation, heme binding analysis, NMR protocols, and fibril density analysis. This material is available free of charge via the Internet at http://pubs.acs.org.

References

(1) MacPhee, C. E.; Dobson, C. M. *J. Am. Chem. Soc.* **2000**, *122*, 12707−12713.
(2) Reches, M.; Gazit, E. *Science* **2003**, *300*, 625−627.
(3) Scheibel, T.; Parthasarathy, R.; Sawicki, G.; Lin, X. M.; Jaeger, H.; Lindquist, S. L. *Proc. Natl. Acad. Sci. U.S.A.* **2003**, *100*, 4527−4532.
(4) MacPhee, C. E.; Woolfson, D. N. *Curr. Opin. Solid State Mater. Sci.* **2004**, *8*, 141−149.
(5) Baxa, U.; Speransky, V.; Steven, A. C.; Wickner, R. B. *Proc. Natl. Acad. Sci. U.S.A.* **2002**, *99*, 5253−5260.
(6) Sondheimer, N.; Lindquist, S. *Mol. Cell.* **2000**, *5*, 163−172.
(7) Leys, D.; Scrutton, N. S. *Curr. Opin. Struct. Biol.* **2004**, *14*, 642−647.
(8) Dobson, C. M. *Nature* **2003**, *426*, 884−890.
(9) Bader, R.; Bamford, R.; Zurdo, J.; Luisi, B. F.; Dobson, C. M. *J. Mol. Biol.* **2006**, 189−208.
(10) Gouterman, M.; Dolphin, D. In *The Porphyrins*; Academic Press: New York, 1978; Vol. 3, pp 1−165.
(11) Christodoulou, J.; Larsson, G.; Fucini, P.; Connell, S. R.; Pertinhez, T. A.; Hanson, C. L.; Redfield, C.; Nierhaus, K. H.; Robinson, C. V.; Schleucher, J.; Dobson, C. M. *Proc. Natl. Acad. Sci. U.S.A.* **2004**, *101*, 10949−10954.
(12) Tanford, C. *Physical Chemistry of Macromolecules*; John Wiley and Sons: New York, 1961.
(13) Page, C. C.; Moser, C. C.; Chen, X.; Dutton, P. L. *Nature* **1999**, *402*, 47−52.

JA0565673